

Temperature-Dependent Charge Carrier Diffusion in $[000\bar{1}]$ Direction of GaN Determined by Luminescence Evaluation of Buried InGaN Quantum Wells

Carsten Netzel,* Veit Hoffmann, Jens W. Tomm, Felix Mahler, Sven Einfeldt, and Markus Weyers

Temperature-dependent transport of photoexcited charge carriers through a nominally undoped, c-plane GaN layer toward buried InGaN quantum wells is investigated by continuous-wave and time-resolved photoluminescence spectroscopy. The excitation of the buried InGaN quantum wells is dominated by charge carrier diffusion through the GaN layer; photon recycling contributes only slightly. With temperature decreasing from 310 to 10 K, the diffusion length in $[000\bar{1}]$ direction increases from 250 to 600 nm in the GaN layer. The diffusion length at 300 K also increases from 100 to 300 nm when increasing the excitation power density from 20 to 500 W cm⁻². The diffusion constant decreases from the low-temperature value of ~ 7 to 1.5 cm² s⁻¹ at 310 K. The temperature dependence of the diffusion constant indicates that the diffusivity at room temperature is limited by optical phonon scattering. Consequently, higher diffusion constants in GaN-based devices require a reduced operation temperature. To increase diffusion lengths at a fixed temperature, the effective recombination time has to be prolonged by reducing the number of nonradiative recombination centers.

quantum wells (QWs). The p-side GaN waveguide in laser diodes is usually undoped to minimize modal absorption induced by Mg acceptors. Accordingly, injection of holes into the QWs is limited and can only be optimized by improving the purity of the GaN crystal and reducing the density of crystal defects.

The diffusion length and the diffusion constant in GaN have already been studied extensively. This includes dependencies on the threading dislocation density,^[2] doping concentration,^[3–5] sample temperature,^[6,7] excitation power,^[3,7] and crystallographic direction.^[8] Measurement techniques are also manifold reaching from photoluminescence (PL)^[3,9–12] and cathodoluminescence^[3,4,13] over light-induced transient grating formation^[2,6,7,14] to electron beam-induced current,^[15,16] photovoltage,^[5] and photoinduced current measurements.^[17]

In this study, the diffusion length and the diffusion constant in unintentionally doped GaN in $[000\bar{1}]$ direction are investigated in the whole temperature range between 10 and 310 K by continuous-wave (cw) and time-resolved photoluminescence (TRPL). The PL intensity from InGaN QWs positioned below the optically excited GaN layer is used to study the charge carrier diffusion process through the GaN. The process which limits diffusion at room temperature or device operation temperature is identified and parameters which can increase charge carrier diffusion in devices are discussed. The results shall contribute to the understanding and the optimization of injection efficiencies in GaN waveguide structures for blue-violet laser diodes.

1. Introduction

High charge carrier diffusivity and long diffusion lengths are important for the performance of GaN-based electronic and optoelectronic devices. In GaN/AlGaIn-based transistor structures, a high lateral electron mobility allows for high-frequency operation. A high hole mobility in $[000\bar{1}]$ direction in p-side GaN waveguide layers of GaN/InGaIn-based laser diodes supports the function of generally applied electron blocking layers.^[1] It increases the injection efficiency of charge carriers into the

2. Results and Discussion

2.1. Experimental Approach

CW PL measurements with excitation and detection via the c-plane surface were performed on samples with top GaN layer thicknesses of 150, 300, and 450 nm above InGaIn QWs to investigate the transport of excited charge carriers into the QWs. In addition, a 15 nm-thick AlGaIn diffusion blocking layer was inserted between the top GaN layer and the InGaIn QWs in a sample with 450 nm-thick top GaN layer. The purpose of the blocking layer is to distinguish between the pumping of the

Dr. C. Netzel, Dr. V. Hoffmann, Dr. S. Einfeldt, Prof. M. Weyers
Ferdinand-Braun-Institut, Leibniz-Institut für Höchstfrequenztechnik
Gustav-Kirchhoff-Straße 4, 12489 Berlin, Germany
E-mail: Carsten.netzel@fbh-berlin.de

Dr. J. W. Tomm, F. Mahler
Max-Born-Institut für Nichtlineare Optik und Kurzzeitspektroskopie
Max-Born-Straße 2A, 12489 Berlin, Germany

 The ORCID identification number(s) for the author(s) of this article can be found under <https://doi.org/10.1002/pssb.202000016>.

© 2020 The Authors. Published by WILEY-VCH Verlag GmbH & Co. KGaA, Weinheim. This is an open access article under the terms of the Creative Commons Attribution License, which permits use, distribution and reproduction in any medium, provided the original work is properly cited.

DOI: 10.1002/pssb.202000016

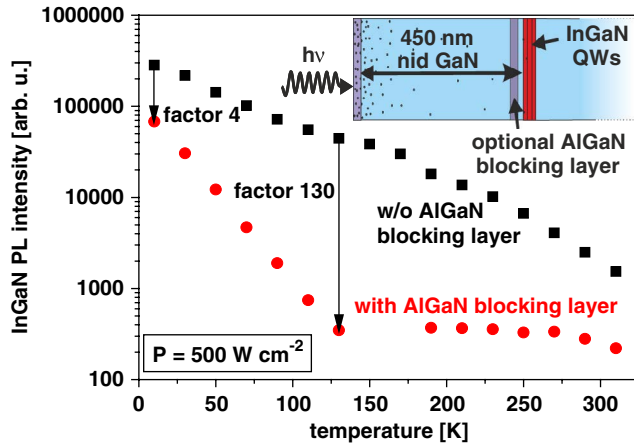


Figure 1. Temperature-dependent cw PL intensity from InGaN QWs located beneath a 450-nm-thick top GaN layer either with (red points) or without (black squares) an $\text{Al}_{0.15}\text{Ga}_{0.85}\text{N}$ diffusion blocking layer between the top GaN layer and the QWs. With a blocking layer and below 150 K, excitation of the QWs is only based on photon recycling. Without a blocking layer, excitation of the QWs is based on photon recycling and charge carrier diffusion through the top GaN layer. The inset shows a sketch of the heterostructure.

QWs by charge carrier diffusion or by reabsorption of PL emitted by the top GaN (compare inset of **Figure 1**). The samples were grown by metalorganic vapor phase epitaxy (MOVPE) on 6 μm -thick (Al)GaN/sapphire buffers at growth conditions typically used for the growth of complete laser structures. A HeCd laser with 325 nm wavelength was used to excite electron–hole pairs near the sample surface with an exponential spatial distribution defined by the absorption coefficient of $1.2 \times 10^5 \text{ cm}^{-1}$ in GaN.^[18] Eighty-five percent of the laser light is absorbed within the first 150 nm of the heterostructure. The excited charge carriers either recombine radiatively or nonradiatively in the GaN layer or diffuse to the InGaN QWs where they can be captured. The PL intensity from the InGaN QWs is then a measure for the number of electrons and holes that reach the QWs.

2.2. Diffusion Length

Figure 1 shows the temperature-dependent PL intensities from the buried InGaN QWs for two samples with and without AlGaN diffusion blocking layer between the 450 nm-thick top GaN layer and the QW region. As the blocking layer should suppress charge carrier diffusion from the optically excited top GaN layer toward the QWs, the remaining InGaN PL intensity is related to other transport processes, e.g., photon recycling of the GaN emission. Figure 1 shows that in the whole temperature range between 10 and 310 K the InGaN PL intensity is much lower if the diffusion blocking layer is present. Accordingly, reabsorption of the GaN emission at the InGaN QWs contributes only little to their population. At 10 K reabsorption processes are responsible for about 25% of the emission intensity from the QWs. This value decreases strongly with increasing temperature because the radiative recombination efficiency in the GaN layer decreases. Consequently, charge carrier diffusion toward the InGaN QWs

is the dominating transport process in samples without a blocking layer and it is legitimate to use the InGaN intensity data to calculate the diffusion length in the top GaN layer in the following sections.

The QW PL intensity for the sample with blocking layer becomes constant at temperatures above 200 K, whereas it decreases further on a higher level for samples without blocking layer. Presumably, the increased thermal energy of charge carriers supports transport over the AlGaN diffusion blocking layer into the QWs in this temperature range. This effect superimposes a further decrease in the InGaN intensity by increased nonradiative recombination which is observed for all other samples without diffusion blocking layer.

Figure 2 shows the temperature-dependent intensities of the InGaN QW emission and the GaN emission from samples with different top GaN layer thicknesses without diffusion blocking layer. Except for the case of the thickest top GaN layer at the highest temperature the InGaN PL intensity is much higher than the GaN intensity. Either the diffusion length in the GaN is larger than the top GaN layer thickness, or differences in the radiative or nonradiative recombination rates between the GaN layer and the InGaN QWs are responsible. All intensities in **Figure 2** decrease with increasing temperature due to thermally activated nonradiative recombination processes. However, the slopes of the curves and the absolute intensity values vary between GaN and InGaN emissions and between samples with different top GaN layer thicknesses.

The GaN emission is weaker in case of a thinner top GaN layer because a greater amount of charge carriers is captured by the InGaN QWs before they can recombine in the initially excited top GaN layer. Accordingly, the InGaN PL intensity is higher for those samples. The GaN PL intensities for the samples with different top GaN layer thickness converge at higher temperatures. Around room temperature, the difference among the samples, namely, the capture of charge carriers into the InGaN QWs, becomes more and more irrelevant for the recombination in the top GaN layer. Concurrently, the InGaN PL intensities diverge with increasing temperature. This behavior shows that the charge carrier diffusion length in the top GaN layer decreases with increasing temperature. The InGaN PL intensity

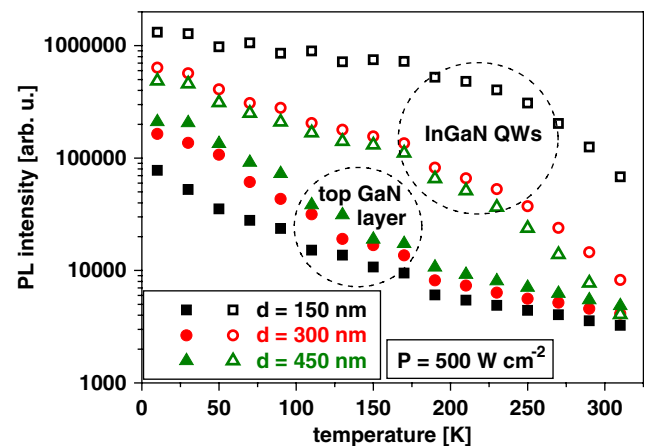


Figure 2. Temperature-dependent GaN and InGaN PL intensity data from cw PL for different top GaN layer thicknesses, d .

depends exponentially on the distance which the carriers have to travel to reach QWs in different depth, i.e.

$$I(d + \Delta d) = I(d) \cdot \exp\left(-\frac{\Delta d}{L_{\text{diff}}}\right) \quad (1)$$

Equation (1) is based on the steady-state solution of the 1D diffusion equation assuming that $d \gg \alpha^{-1}$, $d \gtrsim L_{\text{diff}}$, and $I \sim n$. $I(d)$ are QW PL intensity values, d and $d + \Delta d$ are the depths of the QWs for different samples, α is the absorption constant, n is the density of minority charge carriers which reach the QWs, and L_{diff} is the diffusion length. Proof of the applicability of Equation (1) for the given PL experiments and information about limits of its applicability are given by numerical solutions of the diffusion equation in the Supporting Information. When plotting the logarithm of the InGaN PL intensity values against the depth in which the QWs are located, the slope of a linear fit provides the diffusion length. This evaluation was used to calculate the temperature-dependent charge carrier diffusion lengths in [000 $\bar{1}$] direction in the top GaN layer. Intensity values from the samples with 300 and 450 nm top GaN layer were used. Data from the sample with 150 nm top GaN layer were omitted because the absorption profile already overlapped the InGaN QWs considerably. Direct excitation in the QWs and increasing violation of the conditions for the applicability of Equation (1) makes an evaluation much more complex in this case. The determined temperature-dependent diffusion lengths are shown in **Figure 3a**. Between 10 and 170 K, the diffusion length is around 500–800 nm. The data scattering in this temperature range results from the small differences in the InGaN PL intensity between samples with different thicknesses of the top GaN layer. Therefore, instabilities in the PL intensity measurements, e.g., by the excitation laser, or misalignments of the optics setup have a relatively strong impact on the fitted L_{diff} . Above 170 K, the differences in the InGaN PL intensity between the samples are more pronounced and the diffusion length can be determined more accurately. It decreases down to about 250 nm at 310 K. The diffusion length determined at 300 K for different excitation power densities is shown in **Figure 4**. It decreases by more than a factor of 3 when the excitation power is reduced by one and a half order of magnitudes.

Values for the diffusion length in GaN which can be found in the literature vary strongly. Reported room temperature values for MOVPE-grown GaN on sapphire substrates, in parts also determined by PL spectroscopy, are between 50 and 300 nm.^[9,10,12,14–16] Larger values of 1–3 μm were determined on bulk-like GaN grown by hydride vapor phase epitaxy (HVPE)^[7,19] or for thin layers when the impurity level was sufficiently low.^[5] The diffusion length also seems to depend slightly on the crystallographic direction.^[8] The room temperature diffusion length determined in the current study fits well to the formerly reported values. CL measurements performed at low temperatures have indicated diffusion lengths in the range of 50–500 nm, depending on material quality and crystal orientation.^[3,4,8,13] The low-temperature values observed in this study fit to the upper limit of this range. Concerning the strong excitation power dependence of L_{diff} in **Figure 4**, it has to be kept in mind that the point defect density and accordingly the trap density in unintentionally doped GaN grown by MOVPE is

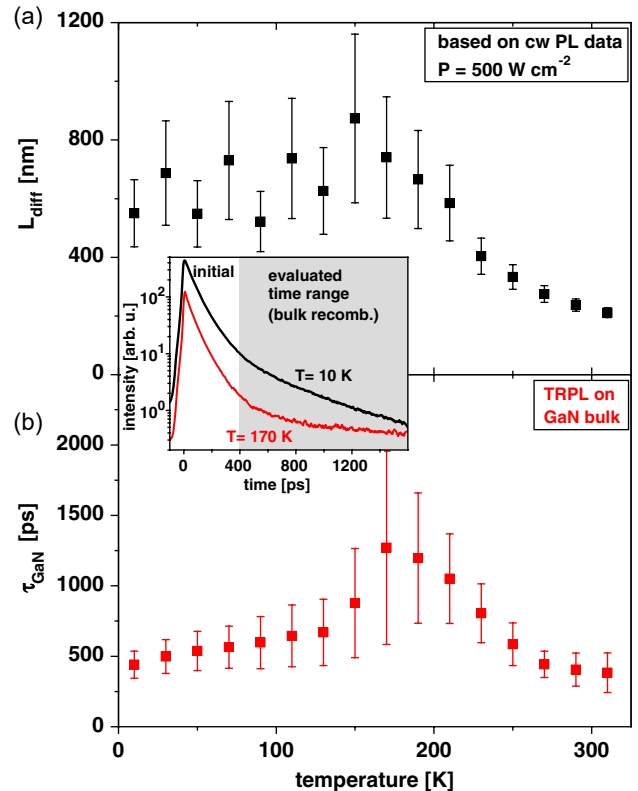


Figure 3. a) Charge carrier diffusion lengths in [000 $\bar{1}$] direction in GaN determined from InGaN PL intensity data of **Figure 2** ($d = 300$ and 450 nm) and b) effective recombination times from a thick bulk-like GaN layer determined 400–1600 ps after the excitation pulse in TRPL. Error bars are based on the stability of the excitation and on the reproducibility of optics adjustment during cw PL intensity measurements for the diffusion length and on the nonexponential temporal luminescence decay for GaN. The inset shows examples of the nonexponential luminescence decay from GaN.

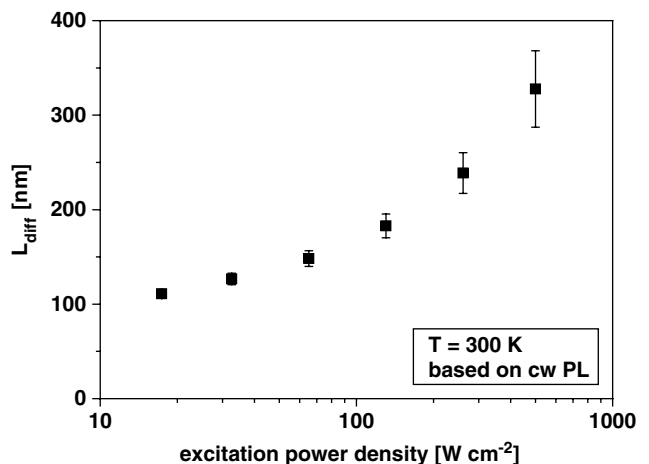


Figure 4. Charge carrier diffusion lengths in [000 $\bar{1}$] direction in GaN in dependence on excitation power density in PL. The values are determined by evaluation of InGaN PL intensities for samples with $d = 300$ and 450 nm.

typically around 10^{16} cm^{-3} .^[20,21] In our PL experiments, the steady-state excess charge carrier density was varied by the excitation power in a very low-density regime, between 10^{14} cm^{-3} and approximately 10^{15} cm^{-3} , i.e., around the expected density of point defects and possible trap states. This circumstance may explain the observed strong excitation power dependence of the diffusion length. Other studies, dealing with significantly higher power densities, have not observed such a strong excitation power dependence of L_{diff} .^[9] Between 20 and 130 K, an almost temperature-independent diffusion length was also observed by Ino et al. in CL experiments at threading dislocations.^[4] However, to the best of our knowledge detailed temperature-dependent measurements of the diffusion length between cryogenic temperatures up to room temperature for MOVPE-grown GaN have not been reported up to now.

2.3. Diffusion Constant

The diffusion constant, D , can be determined from the diffusion length according to Equation (2) which follows from the solution of the diffusion equation

$$D = \frac{L_{\text{diff}}^2}{\tau_{\text{GaN}}} \quad (2)$$

where τ_{GaN} is the effective recombination time in GaN. As the recombination time in the investigated heterostructures is shortened by the charge carrier loss process to the InGaN QWs, luminescence decay times from these samples cannot be used in Equation (2). Therefore, the effective recombination time was determined by TRPL between 10 and 310 K for a 5 μm -thick unintentionally doped GaN layer on sapphire substrate, which was grown under similar conditions as the top GaN layer in the analyzed heterostructures. The decay curves of the bulk GaN luminescence intensity showed the typical deviation from a monoexponential behavior (inset with examples in Figure 3) which also varied with temperature. Effective recombination times were fitted to the tails of these decay curves, following several discussions in literature.^[10,22–25] Hot carrier diffusion and surface recombination, which determine the luminescence decay in the first picoseconds after the excitation pulse, cause the initial short recombination times measured in TRPL. These fast processes become negligible after several hundred picoseconds when diffusion into the bulk has proceeded sufficiently and charge carriers have reached the InGaN QWs. Accordingly, the long recombination times derived from the tail of the decay curves should provide accurate information about recombination processes in the bulk material. The respective recombination times, averaged for the time interval 400–1600 ps after the excitation pulse, are shown in Figure 3b. The error bars show the uncertainty in the derived effective decay times due to the still slightly nonexponential decay behavior in the analyzed time interval.

Figure 5 shows the temperature-dependent diffusion constant in $[000\bar{1}]$ direction for GaN on sapphire (black squares) calculated from the diffusion length and the effective recombination time shown in Figure 3. Below 170 K, the diffusion constant is about $7 \text{ cm}^2 \text{ s}^{-1}$ and it decreases to about $1.5 \text{ cm}^2 \text{ s}^{-1}$ at room temperature. In an independent experiment, values of around

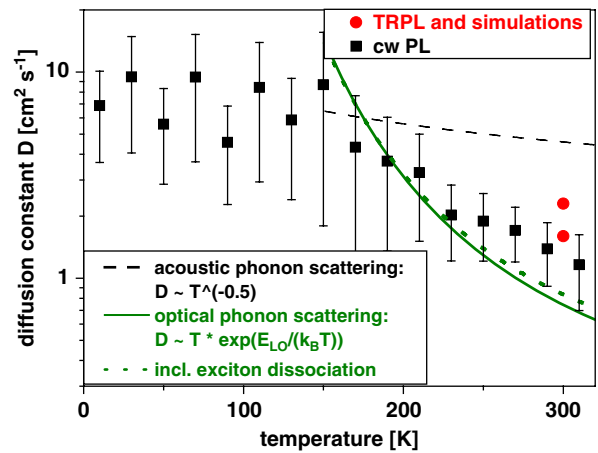


Figure 5. Temperature dependence of the diffusion constant in $[000\bar{1}]$ direction in GaN determined by cw PL (black squares) and by evaluation of the delayed InGaN luminescence intensity dynamics in TRPL measurements at room temperature (red circles). In addition, theoretical temperature dependencies of the diffusion constant from optical phonon scattering (green straight line), optical phonon scattering and exciton dissociation (green dotted line), and acoustic phonon scattering (black dashed line) processes are shown, normalized to $D = 7 \text{ cm}^2 \text{ s}^{-1}$ at $T = 175 \text{ K}$.^[28,29]

$2 \text{ cm}^2 \text{ s}^{-1}$ at 300 K have been determined (red circles) by evaluating TRPL data from the InGaN QW emission of the heterostructures with GaN cap layer thicknesses of 300 and 450 nm, as shown in Figure 6. The data show the delayed onset of the InGaN emission in case of a thicker top GaN layer due to diffusion. Following the approach of Olaizola et al.,^[10] the experimental data were fitted based on a set of rate equations considering the initial excitation profile, diffusion, and recombination

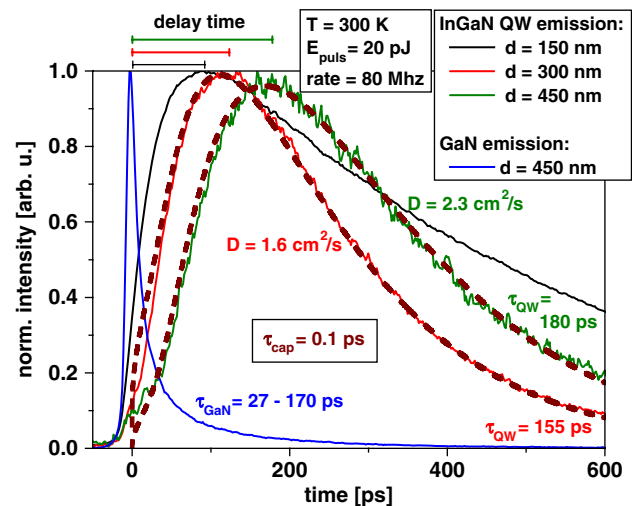


Figure 6. Room temperature TRPL decay curves from InGaN QWs with different top GaN layer thickness, d , and from a top GaN layer for comparison. Dashed brown lines show fits to the experimental data for $d = 300 \text{ nm}$ and 450 nm based on solutions of rate equations for diffusion and recombination in the studied heterostructures.^[10] Given values are results from the fits (D , τ_{QW}) or are input data (τ_{GaN} , τ_{cap}) to the simulations.

in the top GaN layer, capturing of charge carriers into the QWs as well as recombination in the QWs (compare also the Supporting Information). The fits (dashed lines in Figure 6) describe the experimental data very well. The slightly higher diffusion constants in the TRPL experiment may be related to several effects. Small differences in the excitation power density between PL and TRPL cannot be ruled out, especially if trapping of charge carriers is concerned in this low excitation power regime. In addition, in the cw PL experiments, diffusion is measured in the field-free range 300–450 nm below the surface. In TRPL, diffusion is determined from the same range but extended by the surface depletion region and the AlGaIn/GaN interface near the surface.

The determined diffusion constants shown in Figure 5 agree with previously published values. Olaizola et al. and Kuokstis et al. reported a room temperature diffusion constant in $[000\bar{1}]$ direction of $2 \text{ cm}^2 \text{ s}^{-1}$ for GaN grown on sapphire.^[10,23] Mickevičius et al. presented room temperature values of around $1.5 \text{ cm}^2 \text{ s}^{-1}$ for the diffusion in the (0001) plane of GaN on sapphire with varying quality.^[2] Ščajev et al. determined (0001) plane diffusion constants between 0.8 and $1.5 \text{ cm}^2 \text{ s}^{-1}$ at room temperature for thick bulk-like GaN layers from HVPE.^[7] In the same publication, these authors also determined diffusion constants in the (0001) plane between 80 K and room temperature and observed a similar temperature dependence around room temperature as reported here. However, to the best of our knowledge, temperature-dependent diffusion constants in $[000\bar{1}]$ direction for MOVPE grown GaN layers are published for the first time in the present study. In addition, different temperature dependences of the diffusion constant in the temperature ranges below and above 170 K are shown for the first time, here.

2.4. Diffusion-Limiting Processes

The decrease in the diffusion constant between 170 K and room temperature corresponds to scattering of carriers by optical phonons (see theoretical curves in Figure 5). This scattering mechanism is expected to be dominant in ionic crystals around room temperature.^[26] Ščajev et al. concluded from their temperature-dependent measurements (diffusion in (0001) plane, HVPE-grown GaN), too, that diffusion is limited by optical phonon scattering around room temperature.^[7] The temperature dependence of the scattering process should be similar for electrons, holes, and excitons.^[27] Only the absolute scattering rate should vary. A much weaker temperature dependence is expected for acoustic phonon scattering (curve also plotted in Figure 5). Impurity scattering would even lead to an increase in the diffusion constant with temperature.^[27,28] These two mechanisms may be responsible for the limitation of the diffusion constant below 170 K. The consequences of a diffusion constant limited by phonon scattering are the following: 1) an increase in the charge carrier diffusivity around room temperature or device operation temperature cannot be realized by an improved purity of the GaN crystal; 2) carrier injection efficiency in light-emitting devices or laser diodes is sensitive to the device operation temperature.

The diffusion length in $[000\bar{1}]$ direction in GaN at room temperature seems to be limited by optical phonon scattering, too. Both the diffusion length and the diffusion constant show

a similar trend in the temperature dependence above 170 K. However, also the recombination time in the GaN layer decreases above 170 K, presumably due to an activation of nonradiative recombination processes, and thus reduces the diffusion length. As the nonradiative recombination rate can be addressed by a reduction of the point defect density, the realization of longer diffusion lengths at room or device operation temperature should be possible by the optimization of the MOVPE growth process.

It is important to discuss in brief the nature of the carriers which diffuse through the GaN layer. The free exciton binding energy in GaN is $\sim 25 \text{ meV}$.^[29] At low temperature and after the initial thermalization to the band edges, mainly excitons should diffuse. When the thermal energy, $k_B T$, increases and approaches the exciton binding energy, excitons should start to dissociate into free electrons and holes. This effect will change recombination and diffusion processes. Its impact on the measured PL intensities should become visible already between cryogenic temperatures and room temperature. The radiative recombination time in GaN bulk should increase.^[30] This effect may contribute to the increase in the effective recombination time observed between 100 and 170 K (compare Figure 3b). When excitons dissociate and diffusion starts to become ambipolar, the effective masses of the diffusing carriers are smaller and the diffusivity should be larger. The effect should attenuate the decrease in the diffusion constant with increasing temperature by optical phonon scattering and would lead to a slightly better fit to the experimental data (dotted line in Figure 5). Overall, some of the features in the temperature-dependent data for recombination time and diffusion constant might be related to exciton dissociation in the GaN material.

3. Conclusion

Diffusion lengths and diffusion constants in $[000\bar{1}]$ direction for GaN on sapphire substrate have been determined in the temperature range 10–310 K by cw PL and TRPL measurements on heterostructures using InGaIn QWs buried below thick GaN layers. Both values are nearly constant around 600 nm and $7 \text{ cm}^2 \text{ s}^{-1}$ below 170 K and decrease to 250 nm and $1.5 \text{ cm}^2 \text{ s}^{-1}$ around room temperature. The strong temperature-dependent decrease in the diffusion constant above 170 K implies that optical phonon scattering limits the diffusivity around room temperature and beyond. In addition, the diffusion length was found to depend strongly on the excitation power density when the excited excess carrier density was varied around 10^{15} cm^{-3} , slightly below the impurity or defect concentrations in GaN.

Increased hole diffusivity or longer diffusion lengths for the optimization of carrier injection in GaN/InGaIn-based blue-violet emitting laser diodes can, in principle, be obtained by reducing the operation temperature of the devices. However, such an approach would be laborious because the whole laser structure design has to be adjusted to the lowered operation temperature. Consequently, only an increase in the effective recombination time in the p-side GaN waveguide by lowering the density of nonradiative recombination centers such as point defects or dislocations remains as realistic approach to increase the hole diffusion length and the hole injection efficiency.

4. Experimental Section

The studied unintentionally doped c-plane GaN layers (room temperature free electron concentration $\sim 10^{16} \text{ cm}^{-3}$) with thicknesses of 150, 300, and 450 nm were grown by MOVPE (precursors: trimethylgallium and ammonia, growth temperature = 1050 °C, pressure = 200 mbar) on identical threefold $\text{In}_{0.1}\text{Ga}_{0.9}\text{N}$ (3.5 nm)/GaN (9 nm) QWs (precursors: triethylgallium, trimethylindium and ammonia, growth temperature = 780 °C, pressure = 200 mbar) with 6 μm -thick buffer structures on 2 in. sapphire substrates in an AIX200/4-RF-S system. The top GaN layer thicknesses were determined in situ by reflectance measurements and checked after growth by secondary electron microscopy and back scattering electron microscopy in cross section geometry. The threading dislocation density in the GaN layers was in the range of a few times 10^6 cm^{-2} . The GaN was capped by a 15 nm-thick $\text{Al}_{0.15}\text{Ga}_{0.85}\text{N}$ layer to ensure stable nonradiative recombination at the top GaN interface during extended measurement periods or for repeated measurements at different temperature or with different excitation power.^[31] The thin cap layer did not affect the experimental results significantly.

Temperature- and excitation power-dependent PL was performed with cw excitation by a 325 nm HeCd laser on a spot size of about 70 μm in diameter with maximum excitation power density incident on the sample surface of approximately 500 W cm^{-2} . The maximum density of excited charge carriers, determined by the excitation power density and measured effective recombination times, was temperature dependent and in the range 10^{15} – 10^{16} cm^{-3} in the GaN top layer and 10^{16} – 10^{17} cm^{-3} in the QWs. These densities were in the range of the background doping and were low enough to exclude significant impact on the optical transition probability by screening of the quantum confined Stark effect (QCSE) or filling of localization sites in the InGaN QWs. The spectra were measured by a fiber-coupled spectrometer with 1.5 nm spectral resolution and with radiometric calibration. During the measurements, the optics were aligned either to the GaN or to the InGaN peak wavelength for the respective intensity measurements. Therefore, the GaN and InGaN intensities, determined by spectral integration over the respective main peak and the associated phonon replica, can be compared directly. The sample temperature was regulated between 10 and 310 K with an accuracy of 0.2 K by a closed-cycle helium cryostat and a heating resistor.

TRPL measurements were conducted using a setup with a 0.3 m imaging monochromator (Acton SP2300) and a streak camera (Hamamatsu C5680-21 with S20 photocathode) in synchro-scan mode. For the excitation, a frequency-tripled Ti:sapphire laser (Spectra-Physics Tsunami) at 266 nm with a repetition rate of 80 MHz and pulse lengths <100 fs was used. The pulse energy was 20 pJ and the excitation spot diameter about 100 μm . The samples were mounted on a cold head of an optical helium closed-cycle cryostat, which allowed a temperature setting from 5 K to room temperature. The temporal resolution of the entire system, defined as the 1/e decay of the impulse response function, was better than 10 ps.

Supporting Information

Supporting Information is available from the Wiley Online Library or from the author.

Acknowledgements

This work was supported in part by the European Fund for Regional Development of the European Union in the framework of the Berlin-Polish joint project “From UV to blue – Reliable laser sources for environmental monitoring (RelyLa),” administrated by the Investitionsbank Berlin within the “Program to promote research, innovation and technologies” (ProFIT) under Contract 10164535 and in part by the German Research Foundation in the Collaborative Research Centre 787.

Conflict of Interest

The authors declare no conflict of interest.

Keywords

diffusion constants, diffusion lengths, gallium nitride

Received: January 7, 2020

Revised: February 28, 2020

Published online: April 2, 2020

- [1] Y.-K. Kuo, Y.-A. Chang, *IEEE J. Quantum Electron.* **2004**, *40*, 437.
- [2] J. Mickevičius, M. S. Shur, R. S. Qhalid Fareed, J. P. Zhang, R. Gaska, G. Tamulaitis, *Appl. Phys. Lett.* **2005**, *87*, 241918.
- [3] S. Hafiz, F. Zhang, M. Monavarian, V. Avrutin, H. Morkoç, Ü. Özgür, S. Metzner, F. Bertram, J. Christen, B. Gil, *J. Appl. Phys.* **2015**, *117*, 013106.
- [4] N. Ino, N. Yamamoto, *Appl. Phys. Lett.* **2008**, *93*, 232103.
- [5] D. G. Zhao, D. S. Jiang, J. J. Zhu Hui Yang, Z. S. Liu, S. M. Zhang, J. W. Liang, X. P. Hao, L. Wei, X. Li, X. Y. Li, H. M. Gong, *Appl. Phys. Lett.* **2006**, *88*, 252101.
- [6] R. Aleksiejūnas, P. Ščajev, S. Nargelas, T. Malinauskas, A. Kadys, K. Jarašiūnas, *Jpn. J. Appl. Phys.* **2013**, *52*, 08JK01.
- [7] P. Ščajev, K. Jarašiūnas, S. Okur, Ü. Özgür, H. Morkoç, *J. Appl. Phys.* **2012**, *111*, 023702.
- [8] M. Hocker, P. Maier, L. Jerg, I. Tischer, G. Neusser, Ch Kranz, M. Pristovsek, C. J. Humphreys, R. A. R. Leute, D. Heinz, O. Rettig, F. Scholz, K. Thonke, *J. Appl. Phys.* **2016**, *120*, 085703.
- [9] G. P. Yablonskii, A. L. Gurskii, V. N. Pavlovskii, E. V. Lutsenko, V. Z. Zubialevich, T. S. Shulga, A. I. Stognij, H. Kalisch, A. Szymakowski, R. H. Jansen, A. Alam, B. Schineller, M. Heuken, *J. Cryst. Growth* **2005**, *275*, e1733.
- [10] S. M. Olaizola, W. H. Fan, S. A. Hashemizadeh, J.-P. R. Wells, D. J. Mowbray, M. S. Skolnick, A. M. Fox, P. J. Parbrook, *Appl. Phys. Lett.* **2006**, *89*, 072107.
- [11] J. Y. Duboz, F. Binet, D. Dolfi, N. Laurent, F. Scholz, J. Off, A. Sohmer, O. Briot, B. Gil, *Mater. Sci. Eng. B* **1997**, *50*, 289.
- [12] Y. Kawakami, K. Nishizuka, D. Yamada, A. Kaneta, M. Funato, Y. Narukawa, T. Mukai, *Appl. Phys. Lett.* **2007**, *90*, 261912.
- [13] M. Godlewski, E. Łusakowska, E. M. Goldys, M. R. Phillips, T. Böttcher, S. Figge, D. Hommel, P. Prystawko, M. Leszczynski, I. Grzegory, S. Porowski, *Appl. Surf. Sci.* **2004**, *223*, 294.
- [14] E. V. Lutsenko, A. L. Gurskii, V. N. Pavlovskii, G. P. Yablonskii, T. Malinauskas, K. Jarašiūnas, B. Schineller, M. Heuken, *Phys. Status Solidi C* **2006**, *3*, 1935.
- [15] Z. Z. Bandić, P. M. Bridger, E. C. Piquette, T. C. McGill, *Appl. Phys. Lett.* **1998**, *92*, 3166.
- [16] E. B. Yakimov, *J. Alloys Compd.* **2015**, *627*, 344.
- [17] D. Wee, G. Parish, B. Nener, *J. Appl. Phys.* **2012**, *111*, 074503.
- [18] J. F. Muth, J. H. Lee, I. K. Shmagin, R. M. Kolbas, H. C. Casey, B. P. Keller, U. K. Mishra, S. P. DenBaars, *Appl. Phys. Lett.* **1997**, *71*, 2572.
- [19] T. Malinauskas, K. Jarašiūnas, M. Heuken, F. Scholz, P. Brückner, *Phys. Status Solidi C* **2009**, *6*, S743.
- [20] D. D. Koleske, A. E. Wickenden, R. L. Henry, M. E. Twigg, *J. Cryst. Growth* **2002**, *242*, 55.
- [21] S. F. Chichibu, A. Uedono, K. Kojima, H. Ikeda, K. Fujito, S. Takashima, M. Edo, K. Ueno, S. Ishibashi, *J. Appl. Phys.* **2018**, *123*, 161413.

- [22] B. Monemar, P. P. Paskov, J. P. Bergman, A. A. Toropov, T. V. Shubina, T. Malinauskas, A. Usui, *Phys. Status Solidi A* **2008**, 245, 1723.
- [23] E. Kuokstis, G. Tamulaitis, K. Liu, M. S. Shur, J. W. Li, J. W. Yang, M. Asif Khan, *Appl. Phys. Lett.* **2007**, 90, 161920.
- [24] Y. Zhong, K. S. Wong, W. Zhang, D. C. Look, *J. Mater. Sci. Mater. Electron.* **2007**, 18, S453.
- [25] K. P. Korona, *Phys. Rev. B* **2002**, 65, 235312.
- [26] M. Grundmann, *The Physics of Semiconductors*, Springer-Verlag, Berlin, Heidelberg **2016**.
- [27] N. N. Zinov'ev, L. P. Ivanov, I. G. Lang, S. T. Pavlov, A. V. Prokashnikov, I. D. Yaroshetskii, *J. Exp. Theor. Phys.* **1983**, 57, 1254.
- [28] K. Seeger, *Semiconductor Physics*, Springer-Verlag, Wien, New York **1973**.
- [29] S. Tripathy, R. K. Soni, H. Asahi, K. Iwata, R. Kuroiwa, K. Asami, S. Gonda, *J. Appl. Phys.* **1999**, 85, 8386.
- [30] A. Dmitriev, A. Oruzhenikov, *J. Appl. Phys.* **1999**, 86, 3241.
- [31] C. Netzel, J. Jeschke, F. Brunner, A. Knauer, M. Weyers, *J. Appl. Phys.* **2016**, 120, 095307.